QUALITATIVE COMPARISON OF 2D AND 3D COMPUTATION OF FLOW FIELD IN THE CONE SHAPED TURBINE NOZZLE

ROMUALD PUZYREWSKI AND PAWEŁ FLASZYŃSKI*

Department of Turbomachinery and Fluid Mechanics,
Mechanical Faculty, Technical University of Gdansk,
Narutowicza 11/12, 80-952 Gdansk, Poland
rpuzyrew@pg.gda.pl
pflaszyn@task.gda.pl

(Received 10 February 2000; revised version received 29 February 2000)

Abstract: The paper presents qualitative comparison of 2D and 3D computation of flow field in the cone shaped turbine nozzle. The calculation yields surface S_2 for a given conical stream surfaces S_1. S_2 stream surface represents curvature of blading passages. This formulation is typical for the inverse problem. Basing on such obtained surface S_2 it is possible to design the shape of the blade. Results of 3D computation by means of FLUENT have been presented and compared with assumptions in 2D model.

Keywords: internal flow, turbomachinery, turbine nozzle, numerical methods

1. Introduction

Different models of turbomachinery stages are in common use in the flow calculation. The numerical procedures lead either to the design or to determining the flow field in the designed blading. From the design point of view both aspects are very important. Here the model of 2D axisymetric has been applied to solve the inverse problem, which means the determining of the geometry of turbine nozzle shaped in the cone flows [1, 2]. Then 3D numerical procedure (FLUENT 5.1) has been applied to determine the flow parameters in the designed blading. The results

* also at: TASK Computer Centre, Narutowicza 11/12, 80-952 Gdansk, Poland

presented here are the preliminary ones due to the fact that not all conditions for strict comparison have been satisfied.

2. Inverse problem of 2D type

Lower order model, as 2D, is easy to handle for the formulation of the inverse problem. Essentially the idea has been described in [1]. Here the main point will be briefly described. The inverse problem is understood here as searching for the shapes of blading for given streamlines in the meridional, averaged circumferentially, cross-sèction. If the shapes of the streamlines in axi-symmetrical non-orthogonal coordinates $x^{(1)}$, $x^{(2)}$, $x^{(3)}$ are given by:

$$r = f(x^{(1)}, x^{(3)}) = r_w + x^{(1)} x^{(3)}, \tag{1}$$

where: $x^{(1)} = const$ along streamline, $x^{(2)} = \phi$ is cylindrical coordinate along circumference, $x^{(3)} = z$ is the axis, and $f(x^{(1)}, x^{(3)})$ is the stream surface function.

Cone shaped flow in meridional cross-section was chosen as it is shown in Figure 1. The streamlines (stream surfaces) were the cones concentrated at the circle of radius r_w. The transformation rules between Cartesian and non-orthogonal system are:

$$\begin{aligned} x &= f(x^{(1)}, x^{(3)}) \cos x^{(2)}, \\ y &= f(x^{(1)}, x^{(3)}) \sin x^{(2)}, \\ z &= x^{(3)}. \end{aligned} \tag{1a}$$

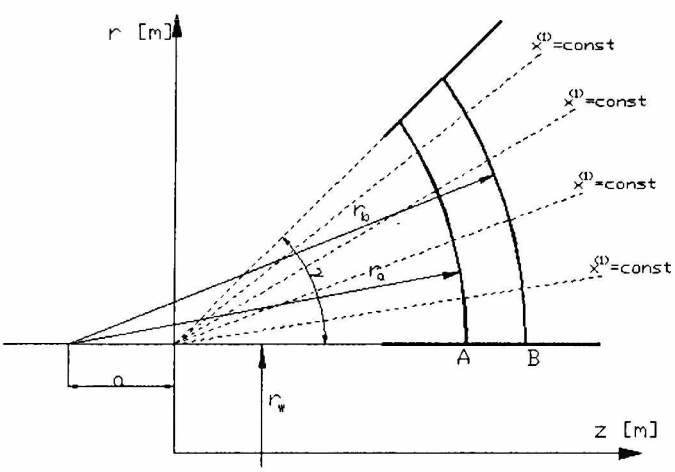

Figure 1. *Stream surfaces in meridional section*

In these coordinates the system governing equations are as follows:

a) mass conservation:

$$\left(1-\tau(x^{(1)},x^{(3)})\right)\rho U_{x3}\frac{f\dfrac{\partial f}{\partial x^{(1)}}}{\sqrt{1+\left(\dfrac{\partial f}{\partial x^{(3)}}\right)^2}}=m(x^{(1)}); \tag{2}$$

b) momentum conservation:

$$-\frac{U_{x2}^2}{f}+\frac{U_{x3}^2\dfrac{\partial^2 f}{\partial\left(x^{(3)}\right)^2}}{1+\left(\dfrac{\partial f}{\partial x^{(3)}}\right)^2}=-\frac{\partial p}{\partial x^{(1)}}\frac{1+\left(\dfrac{\partial f}{\partial x^{(3)}}\right)^2}{\dfrac{\partial f}{\partial x^{(1)}}}+\frac{\partial p}{\partial x^{(3)}}\frac{\partial f}{\partial x^{(3)}}+\rho f_{x1}, \tag{3}$$

$$\frac{U_{x3}}{f\sqrt{1+\left(\dfrac{\partial f}{\partial x^{(3)}}\right)^2}}\frac{\partial(fU_{x2})}{\partial x^{(3)}}=\rho f_{x2}\ , \tag{4}$$

$$\frac{\rho U_{x3}}{\sqrt{1+\left(\dfrac{\partial f}{\partial x^{(3)}}\right)^2}}\left(\frac{\partial U_{x3}}{\partial x^{(3)}}-\frac{U_{x3}}{1+\left(\dfrac{\partial f}{\partial x^{(3)}}\right)^2}\frac{\partial f}{\partial x^{(3)}}\frac{\partial^2 f}{\partial\left(x^{(3)}\right)^2}\right)= \tag{5}$$

$$=\rho f_{x3}+\frac{\partial p}{\partial x^{(1)}}\frac{\dfrac{\partial f}{\partial x^{(3)}}}{\dfrac{\partial f}{\partial x^{(1)}}}\sqrt{1+\left(\frac{\partial f}{\partial x^{(3)}}\right)^2}-\frac{\partial p}{\partial x^{(3)}}\sqrt{1+\left(\frac{\partial f}{\partial x^{(3)}}\right)^2};$$

c) energy conservation along $x^{(1)} = const$:

$$\frac{U^2{}_{x2}+U^2{}_{x3}}{2}+\frac{k}{k-1}\frac{p}{\rho}=e_0\left(x^{(1)}\right); \tag{6}$$

d) Gibbs equation for non-isentropic flow along $x^{(1)} = const$:

$$\rho c_v\frac{dT}{dt}=\frac{p}{\rho}\frac{d\rho}{dt}+\frac{k}{k-1}p\frac{d}{dt}\left(\zeta(x^{(1)},x^{(3)})\left(\left(\frac{p_0}{p}\right)^{\frac{k-1}{k}}-1\right)\right); \tag{7}$$

e) state equation:

$$\frac{p}{\rho}=RT\,, \tag{8}$$

where: U_{x1}, U_{x2}, U_{x3} are the velocity components in the curvilinear system of coordinates, f_{x1}, f_{x2}, f_{x3} are the non-potential body force components in the curvilinear system of coordinates, p is the pressure, ρ is the density, T is the temperature, τ is the blockage factor, ζ is the isentropic loss coefficient and k is the isentropic exponent.

The above set of 7 equations for given $f(x^{(1)}, x^{(3)})$ contains 10 unknown functions:

$$\rho, p, T, U_{x2}, U_{x3}, f_{x1}, f_{x2}, f_{x3}, \zeta, \tau.$$

To close this set of equations three of the above functions have to be predefined. Starting from the generatrix at the inlet, one can find the shape of so called S_2 surface. Surfaces S_2 can be regarded as representatives of the curvature of channels or skeletons of the profiles.

The blockage factor τ and loss coefficient ζ can be chosen as the input data to close the system. The third input is f_{x1} component of body force. This component enables to position the vector of body force $\vec{f}(f_{x1}, f_{x2}, f_{x3})$. If $f_{x1} = 0$, then body force vector is tangential to $x^{(1)} = const$ surfaces, named as S_1 according to [3]. For the case where body force is perpendicular to S_2 one can derive:

$$f_{x1} = -\frac{\sqrt{1+\left(\frac{\partial f}{\partial x^{(3)}}\right)^2}}{\frac{\partial f}{\partial x^{(1)}}}\left(1+\left(\frac{U_{x2}}{U_{x3}}\right)^2\right)U_{x3}\frac{\partial}{\partial x^{(3)}}(fU_{x2})S - \tag{9}$$

$$-\frac{k}{k-1}\frac{p}{\rho}\frac{\sqrt{1+\left(\frac{\partial f}{\partial x^{(3)}}\right)^2}}{\frac{\partial f}{\partial x^{(1)}}}\frac{U_{x2}}{U_{x3}}\frac{\partial}{\partial x^{(3)}}\left(\zeta(x^{(1)}, x^{(3)})\left(\left(\frac{p_0}{p}\right)^{\frac{k-1}{k}}-1\right)\right)fS,$$

where S is the shape parameter determined by the motion of fluid segment on S_2 surface. For the components of segment $(\partial x^{(1)}, \partial x^{(2)}, \partial x^{(3)})$ in its motion along S_2, one can find:

$$S = -\frac{\frac{\partial f}{\partial x^{(1)}}\frac{\partial f}{\partial x^{(3)}}}{\sqrt{1+\left(\frac{\partial f}{\partial x^{(3)}}\right)^2}}\frac{U_{x2}U_{x3}}{f(U_{x2}^2+U_{x3}^2)}+\frac{U_{x3}^2}{U_{x2}^2+U_{x3}^2}\frac{\partial x^{(2)}}{\partial x^{(1)}}- \tag{10}$$

$$-\sqrt{1+\left(\frac{\partial f}{\partial x^{(3)}}\right)^2}\frac{U_{x2}U_{x3}}{f(U_{x2}^2+U_{x3}^2)}\frac{\partial x^{(3)}}{\partial x^{(1)}}.$$

In fact parameter S can be determined after the solution of the system. Therefore the problem is of integral-differential character. If one splits the integral part from the differential part by iterative procedure, the convergence can be reached with a given degree of accuracy. This fact comes out from the numerical solutions performed in the present work. Relation (9) can be rewritten:

$$f_{x1} = \delta(x^{(1)}, x^{(3)})\,(Q_0(p,\rho,U_{x2},U_{x3},S...) + \\ + Q_1(p,\rho,U_{x2},U_{x3},S...)\frac{\partial p}{\partial x^{(3)}} + Q_2(U_{x2},U_{x3},S...)\frac{\partial U_{x2}}{\partial x^{(3)}}), \tag{11}$$

where the parameter δ is the third one to close the system. For $\delta = 0$ there is no component of body force in cross flow direction. For $\delta = 1$ the body force is perpendicular to S_2 surface. The value of δ between 0 and 1 sets up the vector $\vec{f}$ between these two positions. It can be shown that the differential part of the system is of hyperbolical character with two families of characteristics. This leads to two ordinary differential equations. The one is for the characteristic:

$$\frac{dx^{(3)}}{dx^{(1)}} = -\frac{\dfrac{\partial f}{\partial x^{(3)}}\dfrac{\partial f}{\partial x^{(1)}}}{1+\left(\dfrac{\partial f}{\partial x^{(3)}}\right)^2} + \delta\frac{\dfrac{\partial f}{\partial x^{(1)}}}{1+\left(\dfrac{\partial f}{\partial x^{(3)}}\right)^2}\left((D_1 - C_1F_1)\frac{Q_2}{E_1} - \rho Q_1\right), \tag{12}$$

whereas the second one is for the pressure:

$$\frac{dp}{dx^{(1)}} = \frac{\dfrac{\partial f}{\partial x^{(1)}}R_0}{1+\left(\dfrac{\partial f}{\partial x^{(3)}}\right)^2} + \delta\frac{\dfrac{\partial f}{\partial x^{(1)}}}{\left(1+\left(\dfrac{\partial f}{\partial x^{(3)}}\right)^2\right)}\left((R_3 - F_1R_2)\frac{Q_2}{E_1} + \rho Q_0\right), \tag{13}$$

where:

$$Q_0 = -\frac{\sqrt{1+\left(\dfrac{\partial f}{\partial x^{(3)}}\right)^2}}{\dfrac{\partial f}{\partial x^{(1)}}}\frac{U_{x2}}{U_{x3}}fS \times \\ \times\left(\left(1+\left(\frac{U_{x2}}{U_{x3}}\right)^2\right)U_{x3}^2\frac{1}{f}\frac{\partial f}{\partial x^{(3)}} + \frac{k}{k-1}\frac{p}{\rho}\left(\left(\frac{p_0}{p}\right)^{\frac{k-1}{k}} - 1\right)\frac{\partial \zeta}{\partial x^{(3)}}\right), \tag{14}$$

$$Q_1 = \frac{\zeta}{\rho}\left(\frac{p_0}{p}\right)^{\frac{k-1}{k}} \frac{\sqrt{1+\left(\frac{\partial f}{\partial x^{(3)}}\right)^2}}{\frac{\partial f}{\partial x^{(1)}}} \frac{U_{x2}}{U_{x3}} f S, \tag{15}$$

$$Q_2 = \frac{\sqrt{1+\left(\frac{\partial f}{\partial x^{(3)}}\right)^2}}{\frac{\partial f}{\partial x^{(1)}}} \frac{U_{x2}}{U_{x3}} f S \left(-\left(1+\left(\frac{U_{x2}}{U_{x3}}\right)^2\right)\frac{U_{x3}^2}{U_{x2}} + U_w \right), \tag{16}$$

$$\begin{aligned} R_0 &= \frac{\rho U_{x2}^2}{f} - \frac{\rho U_{x3}^2 \frac{\partial^2 f}{\partial\left(x^{(3)}\right)^2}}{1+\left(\frac{\partial f}{\partial x^{(3)}}\right)^2}, \\ R_2 &= -\rho\left(\left(\frac{p_0}{p}\right)^{\frac{k-1}{k}} - 1\right)\frac{\partial \zeta}{\partial x^{(3)}}, \\ R_3 &= -U_{x3}\frac{\partial G}{\partial x^{(3)}}, \end{aligned} \tag{17}$$

$$\begin{aligned} C_1 &= -\frac{\rho}{kp}\left(1+\zeta(k-1)\left(\frac{p_0}{p}\right)^{\frac{k-1}{k}}\right), \\ D_1 &= \frac{k}{k-1}, \\ E_1 &= U_{x2}, \\ F_1 &= \frac{k}{k-1}\frac{p}{\rho} - U_{x3}^2, \end{aligned} \tag{18}$$

$$G\left(x^{(1)}, x^{(3)}\right) = \frac{m\left(x^{(1)}\right)\sqrt{1+\left(\frac{\partial f}{\partial x^{(3)}}\right)^2}}{(1-\tau) f \frac{\partial f}{\partial x^{(1)}}}. \tag{19}$$

The closing functions:

$$\zeta = \zeta(x^{(1)}, x^{(3)}),$$
$$\tau = \tau(x^{(1)}, x^{(3)}),$$
$$\delta = \delta(x^{(1)}, x^{(3)}) \tag{20}$$

are shown in Figures 2, 3 and 4, respectively.

The solution of the inverse problem leads to the shape of blading. For the example considered in [1], the obtained shape of blade has the form shown in Figure 5. The blades as in Figure 5 can be installed in the whole wheel as in Figure 6. This is the geometry for the numerical computation of 3D. The inadequacy of boundary condition consists in the fact that for 2D inverse model the boundary conditions were introduced at the inlet of the nozzle channel, whereas for 3D the inlet and outlet planes were shifted up and down stream of the nozzle profiles.

3. Conditions for 3D computation by FLUENT 5.1

There are 40 blades in cascade configuration with a chord of $c = 0.319\ m$ at the root and $c = 0.384\ m$ at the tip. In order to capture the qualitative features of the flow, a mesh consisting of about 268,000 points has been used.

FLUENT uses a control-volume-based technique to convert the governing equations to algebraic equations that can be solved numerically [4]. The second-order upwind discretization for the convection terms and central-difference scheme for diffusion terms of each governing equation have been applied. SIMPLE algorithm for pressure-velocity coupling in the segregated solver has been used. The calculation has been done using two equations k-e turbulence model (turbulence intensity upstream of the blade 1% and hydra). The boundary conditions are assumed at the inlet ($z00$ – Figure 7) to the computational domain, at the outlet ($z2$), at the walls (blade surface and end walls) and periodic surfaces. Due to the possibility of comparison 2D and 3D results conical flow direction, mass flow rate and total temperature were set at the plane $z00$. The flow direction assumed at the inlet comes directly from 2D model (inverse problem). At the outlet plane the distribution of static pressure was calculated during the convergence procedure from equation:

$$\frac{\partial p}{\partial r} = \frac{\rho U_{\varphi}^2}{r}. \tag{21}$$

For the computation equation of state for the perfect gas has been applied.

The following pictures present pressure distribution (Figure 8) in the whole wheel domain and circumferential velocity in the middle of blade passage (Figure 9). The third one shows almost uniform distribution of outlet angle at section $z1$ (Figure 10), which is calculated from:

$$\tan(alfa) = U_{x3} / U_{x2}, \tag{22}$$

where for 3D model $U_{x3} = \sqrt{U_{axial}^2 + U_{radial}^2}$.

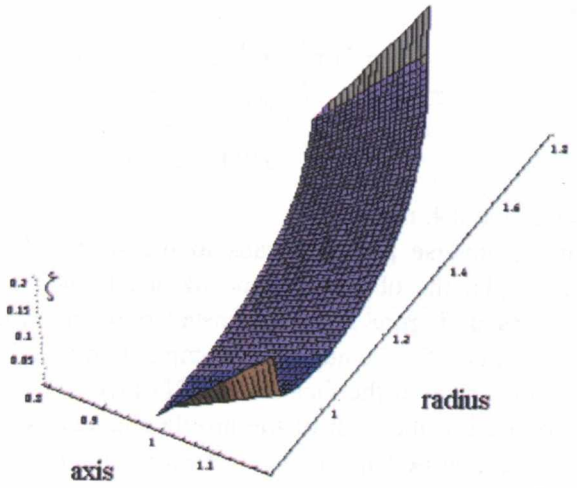

Figure 2. Function ζ

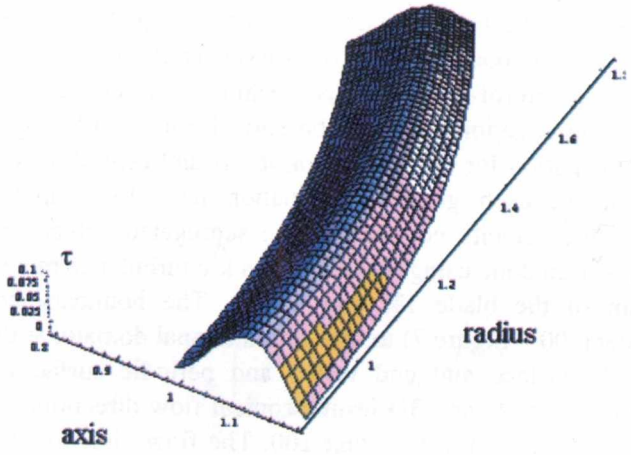

Figure 3. Function τ

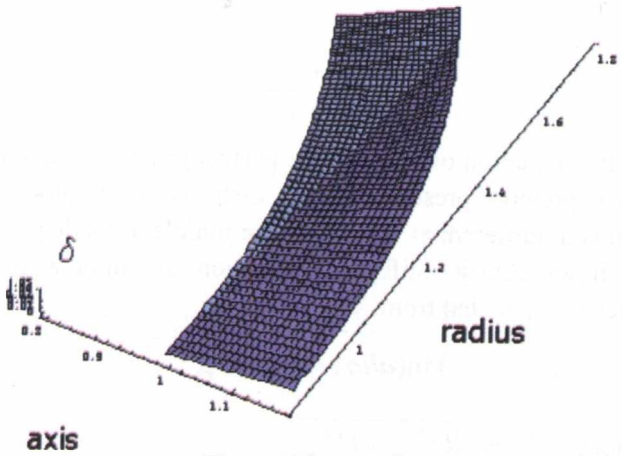

Figure 4. Function δ

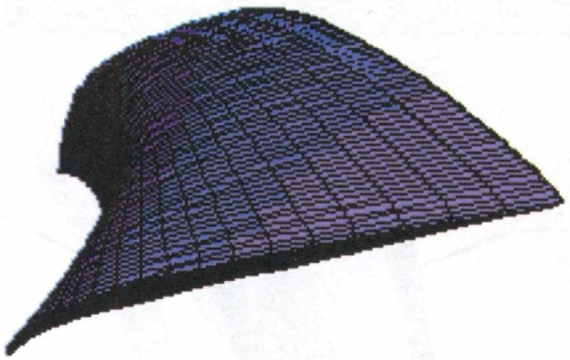

Figure 5. *Stator blade*

Figure 6. *Stator wheel*

This uniformity is the advantage, which comes from highly 3D shape of the nozzle. The distinction between the results obtained by means of 2D and 3D model can arise from one of the main features of the first one (2D) – axisymmetry. In the axisymmetric case, there is an infinitesimal pitch and the flow takes place along stream surfaces S_2, so 3D effects and changes in circumference direction are excluded from consideration.

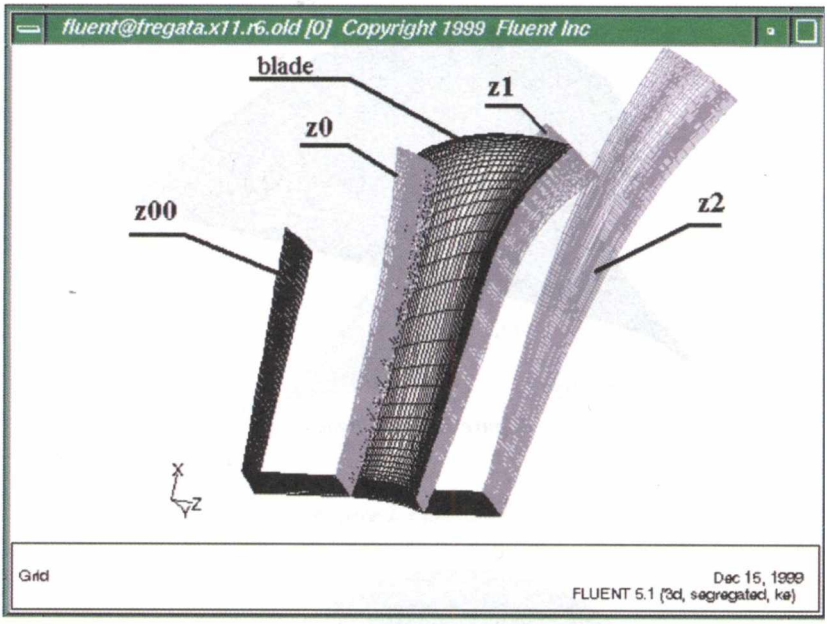

Figure 7. *Control surfaces*

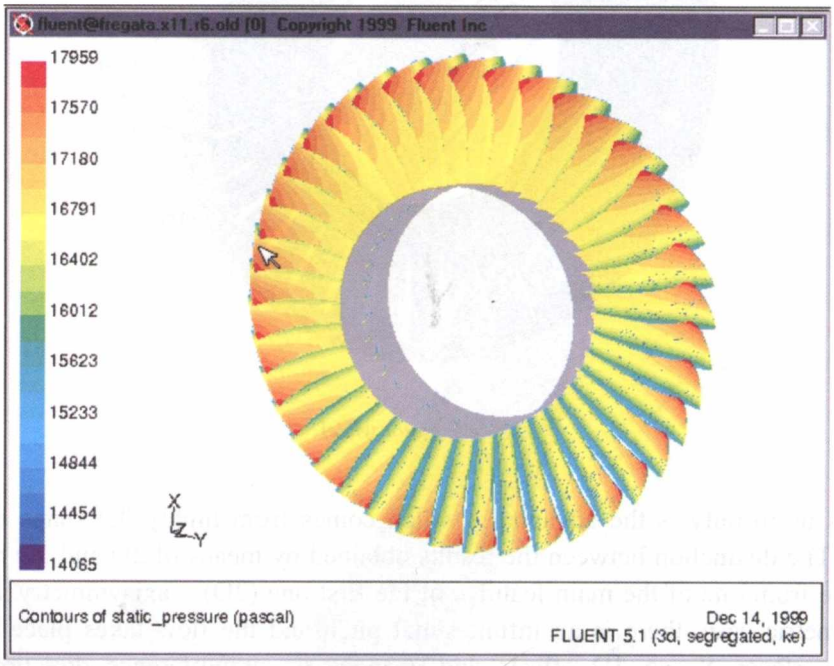

Figure 8. *Pressure distribution in the stator domain*

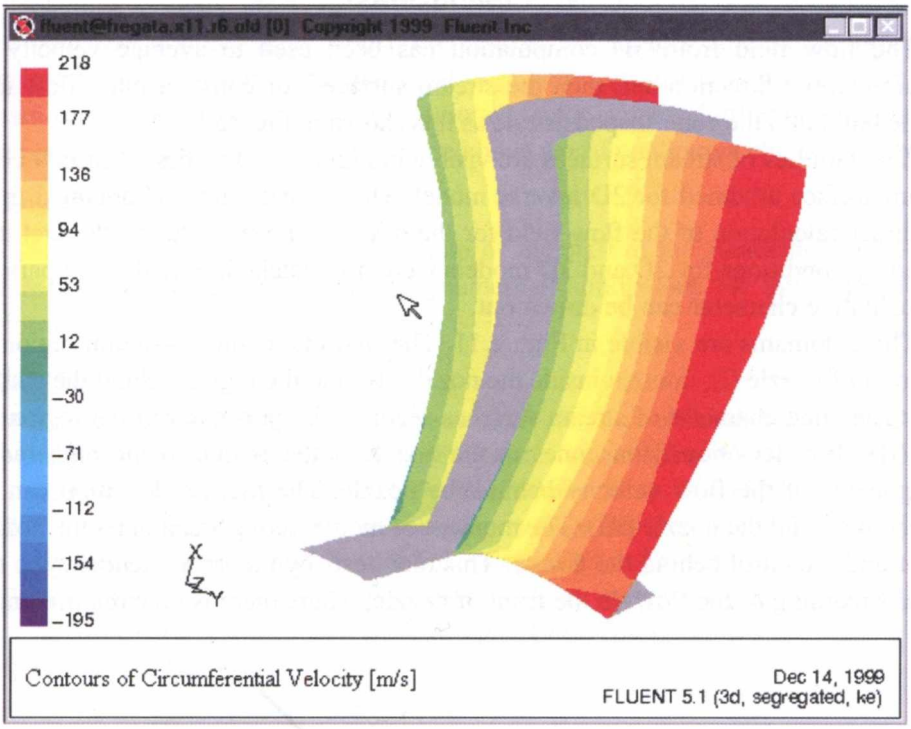

Figure 9. *Circumferential velocity in the middle of the blade passage*

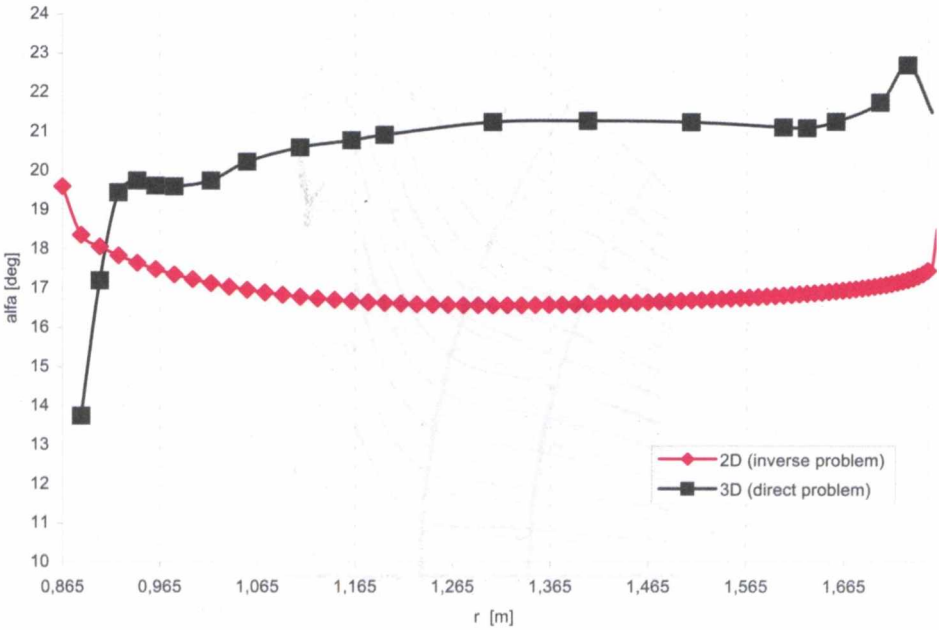

Figure 10. *Flow angle at the section z1*

4. Conclusions

The flow field from 3D computation has been used to average velocity in circumferential direction and then the stream surfaces for constant mass flow rate can be build into the cone shaped nozzle as it is shown in Figure 11.

Two families of stream surfaces are visible in Figure 11. The first is strictly cone stream surface assumed for 2D inverse model. The second family is obtained from 3D direct calculation of the flow field for the designed nozzle. Due to the fact that boundary conditions for 2D and 3D models were not matched, only the comparison of qualitative character can be drawn out.

Three domains are visible in Figure 11. The first one is the up-stream region in the front of nozzle (I), domain inside the nozzle (II) and the region behind the nozzle (III). The cone character of stream surfaces seems to be preserved in the region (I) and (II). The deviation from cones at the nozzle outlet is due to the high radial components of the flow velocity behind the nozzle. The highest deviation can be observed behind the nozzle (III). The moment of momentum generated by the nozzle is not under control behind the nozzle. This manifests by the strong tendency to the radial streaming of the flow. In the front of nozzle, where there is no circumferential

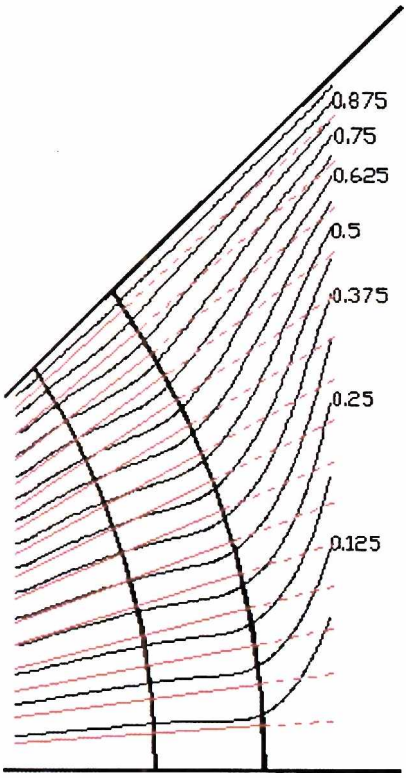

Figure 11. *Two families of stream surfaces in meridional section: conical (red) and averaged 3D results (black)*

component of velocity, the deviation from cone character of the flow, assumed at the inlet boundary conditions, is well preserved. In the authors opinion the properly matched boundary conditions could result in a better quantitative agreement in the stream surface positions. The above mentioned factor is under further investigations. The results presented are the first ones and have are of qualitative character only.

Acknowledgements

The authors are grateful for kind help of the staff at the Academic Computer Centre in Gdansk (TASK), where 3D numerical simulations for this paper were performed.

References

[1] Puzyrewski R and Tesch K., *Sweep Lean, Taper and Twist of Nozzle blading in 2D model Inverse Problem*, Proceedings of International Conference SYMKOM'99, Technical University of Lodz, 1999, Thermal Turbomachines, No. 115 1999

[2] Puzyrewski R., *14 Lectures of Turbomachniery stage theory – 2D model*, Technical University of Gdansk, ABB Zamech Ltd., Gdansk 1998 (in Polish)

[3] Wu C. H., *General theory of three-dimensional flow in subsonic and supersonic turbomachines of axial, radial and mixed flow types*, Trans. ASME 1952

[4] FLUENT 5 User's Guide